

Measuring Characteristics of a Helium-Neon Laser

Adrian deCola*

Physics and Economics Major; Computer Science Minor, Bates College, Lewiston, ME 04240, USA

(Dated: December 30, 2021)

Lasers have many commercial, technological, and research related uses. We explore characteristics of a Helium-Neon laser using a Fabry-Perot interferometer, which was mounted on a PZT crystal, an electromagnet, and an oscilloscope. The laser was pointed towards the Fabry-Perot interferometer and using the oscilloscope, a triangular voltage was applied across the interferometer allowing it to grow and different standing waves to build up in the cavity, allowing us to view the output of the laser against varying frequencies. Using these devices, the laser mode spacing of this He-Ne laser, the width of its gain curve, the speed of the fastest lasing atoms, the PZT crystal length change per volt, the Zeeman splitting vs B constant, and the change in the laser cavity length from room temperature while operating were all calculated. Most uncertainties in these values came from the discretization of the voltages collected from the oscilloscope and the uncertainty in measuring the applied magnetic field.

I. INTRODUCTION AND HISTORY

The word laser has become short hand for light amplification by stimulated emission of radiation. Lasers produce a specific wavelength, or wavelengths, of light, beyond discernible to the naked eye. A Helium-Neon laser uses a gaseous mixture of a 10:1 Helium to Neon ratio. Helium-Neon lasers typically produces light with a wavelength of 632.8 nanometers, appearing red to the human eye. This happens by exciting the electron in the Neon atoms through collisions with Helium atoms, creating a population inversion in the Neon atoms' electron states, where more atoms have electrons in the higher energy state than atoms with electrons in the low energy state. When these electrons lower energy states, they create a chain reaction causing the other electrons to drop energy states, with the released photons in phase and traveling in the same direction. [1]

While the efficiency of most lasers is low, they produce a narrow beam of light, in phase, with a high energy density. For this reason, lasers have many commercial uses. They are used in bar-code readers and CD creation and players. They are also tools for mapping, which has scientific and military purposes. Due to their coherence, lasers can travel large distances and return and still be received. Timing this process allows for mapping of many surfaces. Laser's high energy density's also mean they can be used for cutting and welding materials. Due to their monochromatic, lasers have many scientific and medical uses as well. Lasers can be used to stimulate certain reactions. In addition, laser spectroscopy has many applications in atmospheric physics and diagnosing cancer. [2]

Here we will measure characteristics of a Helium-Neon laser including: its laser mode spacing, the width of its gain curve, the speed of the fastest lasing atoms, the PZT crystal length change per volt, the Zeeman splitting vs B

constant, and the change in the laser cavity length from room temperature while operating for three minutes.

II. THEORY

*Note: All error propagation will be calculated with the following equation.

$$\sigma_V = \sqrt{\sum_i \left(\frac{\partial V}{\partial p_i} \right)^2 \sigma_{p_i}^2} \quad (1)$$

Where V is the value whose uncertainty will be calculated and p_i are its individual components.

To calculate the mode spacing, the time spacing between modes can be compared to the time spacing between repeating mode patterns due to the free spectral range in accordance with the following equation: $\frac{\Delta t}{\Delta T} = \frac{f}{FSR}$ where Δt is the time difference between two lasing mode peaks, ΔT is the time difference to reach another repeating patterns of modes or the amount of time that represents the free spectral range, which is given as 8 GHz, and f is the laser mode spacing.

$$f = \frac{\Delta t}{\Delta T} FSR \quad (2)$$

*Note: This free spectral range applies only to light with wavelengths of light around those produced by a He-Ne laser.

This is the equation we will use to calculate the laser mode spacing. An uncertainty in f can be calculated using error propagation:

$$\sigma_f = \sqrt{\left(\frac{1}{\Delta T} FSR \sigma_{\Delta t} \right)^2 + \left(\frac{-\Delta t}{(\Delta T)^2} FSR \sigma_{\Delta T} \right)^2} \quad (3)$$

An uncertainty in each time is due to the discretization of the data collected.

*Electronic address: adecola@bates.edu

The length of the laser cavity can be calculated from the calculated laser mode spacing to roughly check the calculated laser mode spacing.

$$L = \frac{c}{2f} \quad (4)$$

Using error propagation the uncertainty in this value is

$$\sigma_L = \frac{c\sigma_f}{2f^2} \quad (5)$$

To calculate the width of the gain curve, similar to calculating the laser mode spacing, the time spacing between start and end of each gain curves can be compared to the time spacing between repeating gain curves due to the free spectral range in accordance with the following equation:

$$w = \frac{\Delta t}{\Delta T} FSR \quad (6)$$

where Δt is the time difference between start and end of each gain curves, ΔT is the time difference to repeated gain curves, and w is width of the gain curve, as a range of frequencies. An uncertainty in the gain curve width can be calculated using error propagation.

$$\sigma_w = \sqrt{\left(\frac{1}{\Delta T} FSR \sigma_{\Delta t}\right)^2 + \left(\frac{-\Delta t}{(\Delta T)^2} FSR \sigma_{\Delta T}\right)^2} \quad (7)$$

The frequency shift from the Doppler Effect is what will be used to calculated the speed of the fastest lasing atoms.

$$f' = f \frac{c}{c \pm v} \quad (8)$$

Where f' is the detected frequency of one photon with its source moving at a speed v relative to the Fabry-Perot interferometer and f is the frequency of the photon when its source is not moving relative to the interferometer. The value for the wavelength of a Helium-Neon laser is 632.8nm . There is uncertainty in this value; however it is relatively much smaller than the uncertainty estimated width of the gain curve, so we will treat it as an exact value. From this wavelength the frequency of this light can be calculated, when the source atoms are not moving relative the the Fabry-Perot Spectral Analyser as $f = \frac{c}{\lambda}$. Let's consider the maximum frequency viewed:

$$f_{max} = \frac{c}{\lambda} \frac{c}{c - v_{max}} \quad (9)$$

It is clear that the maximum frequency is the equilibrium frequency when the atoms are not moving relative to the detector plus half of the gain curve width.

$$f_{max} = f + \frac{1}{2}w \quad (10)$$

After simplifying, the following equation is calculated and will be used to calculate the speed of the fastest lasing atoms.

$$v_{max} = c - \frac{c^2}{\lambda(\frac{c}{\lambda} + \frac{1}{2}w)} \quad (11)$$

Using error propagation, the uncertainty in this value is

$$\sigma_{v_{max}} = \frac{c^2}{2\lambda(\frac{c}{\lambda} + \frac{1}{2}w)^2} \sigma_{v_{max}} \quad (12)$$

The PZT length change per Volt is in accordance with the following equation:

$$l = \frac{\Delta L_{PZT}}{\Delta V} = \frac{\Delta L_{PZT}}{V_2 - V_1} \quad (13)$$

This can be calculated using the resonant peaks found in calculating the laser mode spacing and finding the corresponding applied voltages to the PZT crystal. The change in PZT length that corresponds to these resonant frequencies is a half wavelength of the light entering the interferometer. In this case,

$$\Delta L_{PZT} = \frac{\lambda}{2} = 316.4 \text{ nm} \quad (14)$$

The uncertainty in the PZT length change per volt is

$$\sigma_l = \sqrt{\left(\frac{\Delta L_{PZT}}{(V_2 - V_1)^2} \sigma_{V_2}\right)^2 + \left(\frac{\Delta L_{PZT}}{(V_2 - V_1)^2} \sigma_{V_1}\right)^2} \quad (15)$$

An uncertainty in each applied voltage is due to the discretization of the data collected.

The Zeeman splitting vs B constant being measured corresponds to half the energy difference between the two lasing modes. $\Delta E = \frac{1}{2}(E_2 - E_1)$ where E_2 and E_1 are the two 'split' lasing frequencies.

*Note: The energy levels are calculated as frequencies, as they are directly related through Plank's constant.

The proportionality constant, X , is related to this energy difference: $\Delta E = X * B$, where B is the applied magnetic field.

$$X = \frac{\Delta E_{2,1}}{2B} \quad (16)$$

The uncertainty in this value is calculated as follows:

$$\sigma_X = \sqrt{\left(\frac{\sigma_{\Delta E_{2,1}}}{2B}\right)^2 + \left(\frac{\sigma_B \Delta E_{2,1}}{2B^2}\right)^2} \quad (17)$$

To calculate the frequency or energy difference, the frequency spacing of two curves is once again compared to the free spectral range.

$$\Delta E_{2,1} = \frac{\Delta t}{\Delta T} FSR \quad (18)$$

The uncertainty in this energy drop, $\Delta E_{2,1}$, is calculated using error propagation:

$$\sigma_{\Delta E_{2,1}} = \sqrt{\left(\frac{1}{\Delta T} FSR \sigma_{\Delta t}\right)^2 + \left(\frac{-\Delta t}{(\Delta T)^2} FSR \sigma_{\Delta T}\right)^2} \quad (19)$$

When the laser turns on, its cavity begins to warm and expand. This can be viewed as different modes begin to lase. An expression for the change in the laser cavity length over three minutes can be derived from calculating the difference in start and end mode numbers.

$$\Delta L = \frac{\Delta mc}{2f} \quad (20)$$

Using error propagation the uncertainty in this value is

$$\sigma_{\Delta L} = \frac{c \sigma_{\Delta n}}{2f} \quad (21)$$

III. APPARATUS AND PROCEDURE



FIG. 1: A simplified version of the laboratory set-up used.

A setup similar to that shown in Figure 1 was used. A triangular voltage across was applied across the Fabry-Perot interferometer PZT crystal, on which the walls of the cavity were mounted. This caused the cavity to expand linearly and capture different lasing modes as it did so, as different frequencies would build standing waves at different cavity lengths; visible as an output voltage on the oscilloscope.

The oscilloscope had an option to pile peak voltages. Since the laser cavity grew while operating, lasing modes would pass through the gain curve and this oscilloscope function could be used to track the gain curve and its width. This same process was used when a magnetic field was applied to the laser. The magnetic field was

measured as close to the center of the laser as possible where the strongest field was found. Data was collected for a range of fields from 300 to 700 Gauss.

The gain curves contained lots of data as the oscilloscope collected data for long periods of time. However, as the oscilloscope collected more data it marked peak voltage locations and so outliers would become more and more common, though not visible to us. In addition, the time intervals of data collection were still discretized by the same amount no matter how much data we collected for each gain curve. For these reasons, it was still important to preform trials.

IV. OBSERVATIONS AND ANALYSIS

Many activities occurred in the seemingly simple set up shown in Figure 1. One aspect was that there was a Doppler shift in the output of light due to the gas in the laser moving with respect to the interferometer. This meant that multiple modes of light were able to ‘lase’ at the same time: in this case, 2. This is shown in Figure 2 with the calculated peaks used in calculating the laser mode spacing and PZT length change per Volt.

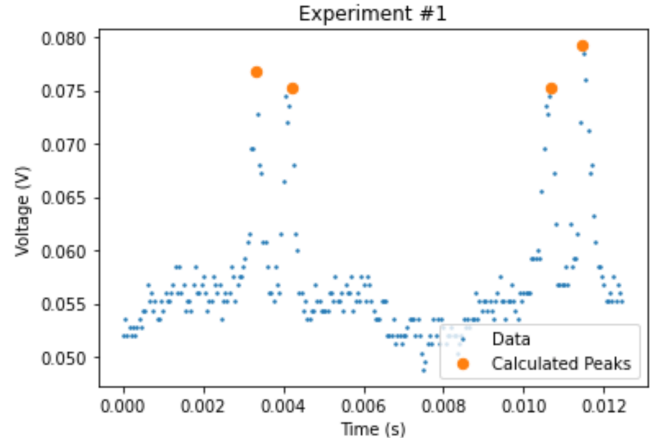


FIG. 2: An example of the data used to calculate the peaks of different lasing modes.

The gas in the laser moved at different speeds and directions relative to the Fabry-Perot interferometer formed a “gain curve,” which was symmetric, but did not have tails on either end. This is shown in Figure 3 the calculated base points to calculate its width and the speed of the fastest lasing atoms.

As the laser ran, the cavity grew due to higher temperatures. This caused different modes to lase: visible as the laser modes traveling across the screen within the gain curve.

If we applied a magnetic field to the laser, the energy levels of the electrons in the Neon atoms would split.

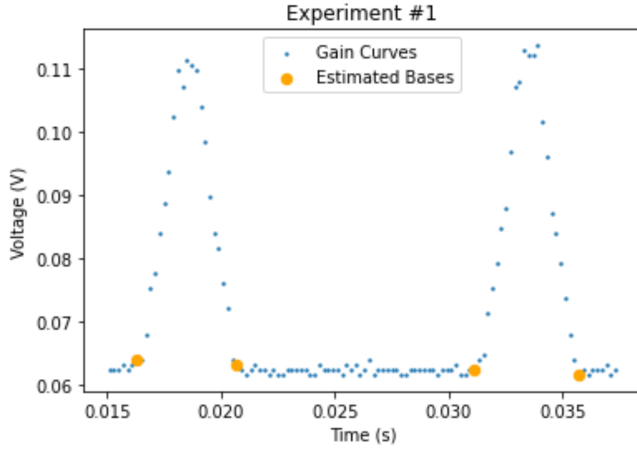


FIG. 3: An example gain curve with its base points calculated.

This meant that multiple frequencies of light corresponding to these energy drops were visible. As the magnetic field was strengthened, the energy levels further split as did the energy drops and light frequencies corresponding to them. This was visible as the gain curves of the corresponding energy drops split further as the magnetic field was increased. An example of these split energy drops is shown in Figure 4 with the calculated peaks used to calculate the Zeeman splitting vs B constant.

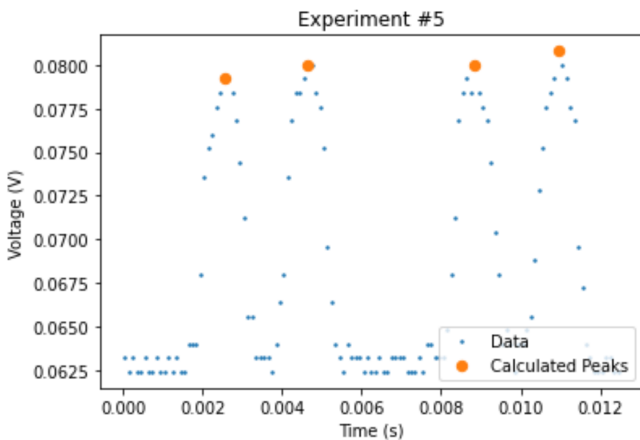


FIG. 4: An example of the different energy drops from an applied magnetic field with its calculated peaks.

V. CONCLUSIONS AND OUTLOOK

Figure 5 shows the calculated values for the laser mode spacing.

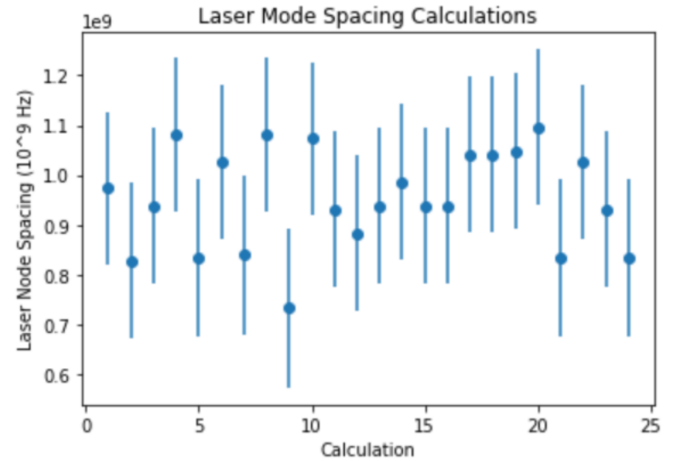


FIG. 5: The calculated laser mode spacing values in Hz.

The weighted average value for the laser mode spacing is $(9.5 \pm 0.3) * 10^8 \text{ Hz}$. The spread calculated value for the laser mode spacing is $(9.5 \pm 0.2) * 10^8 \text{ Hz}$. These two values are in agreement with each other: as reflected in the graph as well, as the spread in the values is proportional to the uncertainty in each value. The data in some collections was noisy and it was hard to estimate peaks-leading to the uncertainty in these estimates. This result can be used to derive a length of the laser cavity of $16 \pm 1 \text{ cm}$. This length is in agreement with the estimated laser cavity length as estimated by eye.

Figure 6 shows calculated values for the width of the gain curve as a frequency.

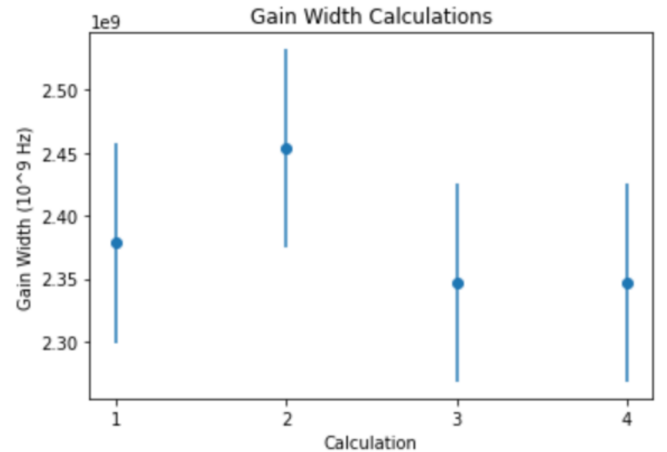


FIG. 6: The calculated values for the width of the gain curve in Hz.

The weighted average value for the width of the gain curve is $(2.38 \pm 0.04) * 10^9 \text{ Hz}$. The spread calculated value for the width of the gain curve is $(2.38 \pm 0.03) * 10^9 \text{ Hz}$. These two values are in agreement with each other. The

uncertainty in this experiment came from the fact that the data collection was discretized and the actual bases of the gain curve could have been anywhere between two of these discretized points. An oscilloscope with more frequent data collection could lower the uncertainty in these estimates for the width of the gain curve. This value gives us a sense of the gain curve widths that would be seen in other Helium Neon lasers, a value that should be small relative to the laser mode spacing if one cares about the amount of wavelengths of light present from a laser.

Figure 7 shows the calculated values for the speed of the fastest lasing atoms.

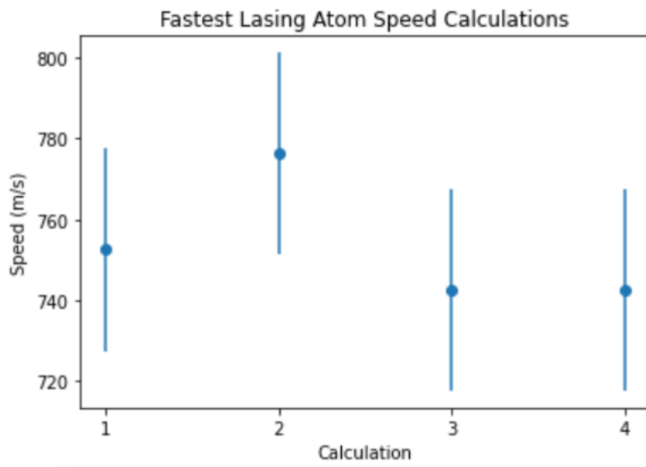


FIG. 7: The calculated speed of the fastest lasing atoms in meters per second.

The weighted average value and spread calculated value for the speed of the fastest lasing atoms are in agreement with each other at $750 \pm 10 \frac{m}{s}$. Uncertainty in these calculations come once again from the fact that the data collection was discretized and the actual bases of the gain curve could have been anywhere between two of these discretized points.

Figure 8 shows the calculated values for the PZT crystal length change per volt.

The weighted average value for the PZT crystal length change per volt is $(9.58 \pm 0.04) * 10^{-7} \frac{m}{V}$. The spread calculated value for the PZT crystal length change per volt is $(9.62 \pm 0.05) * 10^{-7} \frac{m}{V}$. These two values are in agreement with each other. The uncertainties in these values come from trying to estimate the peak of the lasing mode peaks and their corresponding applied voltages. An oscilloscope that collected data more frequently would once again lower these uncertainties. However, there was still noise present in the data that could be overcome with cleaner voltage signals.

Figure 9 shows the calculated values for the Zeeman splitting vs. B constant.

The weighted average value for this constant is $(2.4 \pm 0.06) * 10^6 \frac{Hz}{G}$. The spread calculated value for this con-

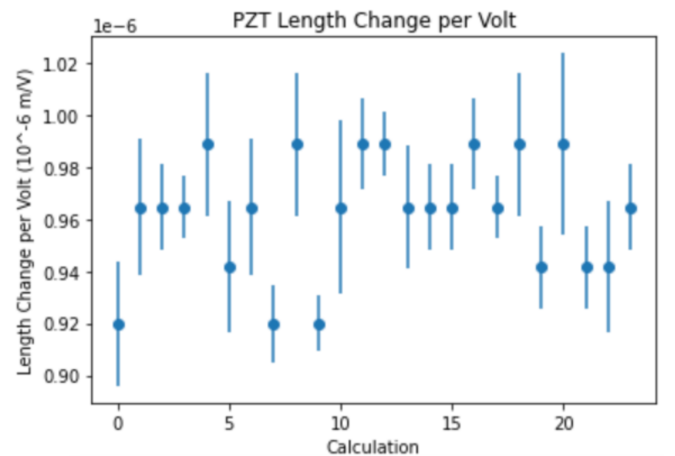


FIG. 8: The calculated values for the PZT crystal length change per volt.

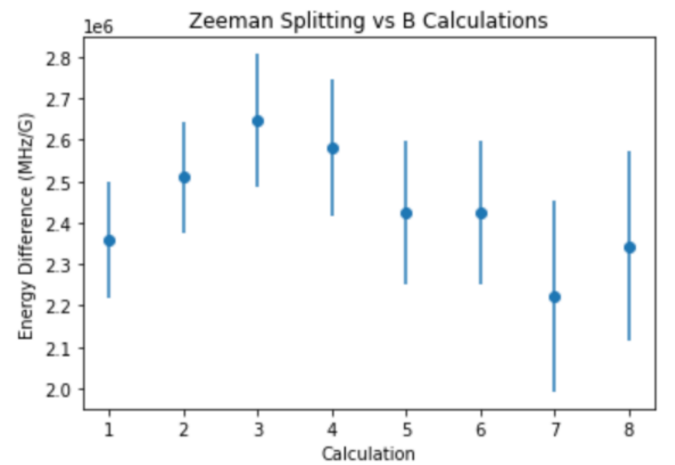


FIG. 9: The calculated values for the constant relating the Zeeman splitting per magnetic field strength applied in Hz per Gauss.

stant is $(2.44 \pm 0.05) * 10^6 \frac{Hz}{G}$. These two values are in agreement with each other. The uncertainties in this value come from estimating the peaks of the gain curves from the energy drops. There is certainly a possibility of systematic errors from the fact that the magnetic field applied to the laser measurements were likely underestimated as it was not possible to measure the magnetic field inside the laser, where it was the strongest. This underestimation in the magnetic field would mean that the true value for this constant is likely smaller than our calculated value.

The change in laser cavity length after three minutes from room temperature is $(7.3 \pm 0.3)\mu\text{m}$. Meaning the laser cavity grew by this value in three minutes. This gives an idea of how much the laser grows by when first

operating. As it was seen that the nodes passed by slower as the laser grew, this meant that the growth of the laser cavity slowed due to the laser approaching its peak operating temperature. This could be important if one is concerned with the intensity and differing wavelengths that could have been used in their experiment to calculate uncertainties. In addition, it could be important if one would like to use frequencies of light that differ only minusculely.

Acknowledgments

Special thanks is given to Biruk Chafamo, Nathan Lundblad, and the Bates Academic Resource Commons for their contributions to this paper.

-
- [1] C. B. Hitz, J. J. Ewing, and J. Hecht, *Introduction to laser technology*, John Wiley & Sons, 2012.
 - [2] K. Shimoda, *Introduction to laser physics*, volume 44, Springer, 2013.